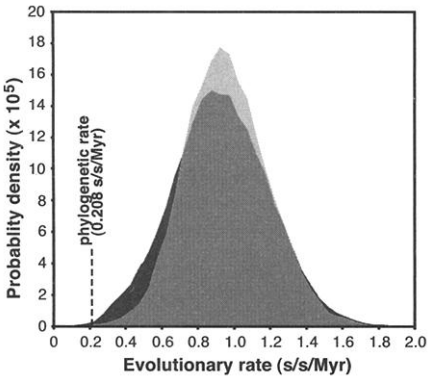

Fig. 3. Posterior probability densities of the evolutionary rate (s/s/Myr) under two models of population dynamics: constant population size (lighter distribution) and exponential growth (darker distribution).

of substitutions per nucleotide site against the time between serially preserved Adélie penguin samples. The regression estimated the rate of HVRI evolution to be 0.676 s/s/Myr; using a parametric bootstrap of 1000 replicates, the 95% confidence intervals were 0 to 2.04 s/s/Myr. The point estimate obtained from this analysis lies well within the two probability distributions obtained from the MCMC analyses. However, the wider confidence interval, which is expected because the method uses only summary distance information and ignores specific site patterns (*18*), does not exclude the phylogenetically derived estimate.

Mitochondrial HVRI sequences from Adélie penguins are evolving in a clock-like manner in that 89% of all samples belonging to the A and RS lineages passed a relative rate test (*19*) and a likelihood ratio test (*20*) ($P > 0.05$) [see the supplemental material (*12*)]. Estimates of the time of divergence of the A and RS lineages were produced by the MCMC analysis. The mean divergence times were 62,000 years (95% HPD interval 32,000 to 95,000) and 53,000 years (95% HPD interval 26,000 to 90,000) for constant and exponential growth, respectively. Both our point estimates and the 95% intervals indicate that the two lineages diverged during the last glacial cycle (*21*, *22*). This is consistent with the fact that at the Last Glacial Maximum, there were few, if any, ice-free areas in the Ross Sea, and Adélie penguins are likely to have been restricted to refugia.

Although other studies have used ancient DNA to document changes in animal populations over time (*23*, *24*), these data sets have not been used to estimate evolutionary rates. The fast evolutionary rate reported here of two to seven times that of the phylogenetic rate is concordant with the high rate of HVRI mutation found recently in humans (*25*). We suggest that an evolutionary rate of the mitochondrial HVRI of 0.4 to 1.4 s/s/Myr is more realistic than previous slower phylogenetic estimates, particularly for intraspecific studies and studies of closely related species. The fact that we have been able to use ancient DNA to measure the tempo of evolution illustrates the importance of these unique Adélie penguin bone deposits.

References and Notes

1. R. L. Cann, M. Stoneking, A. C. Wilson, *Nature* **325**, 31 (1987).
2. G. F. Shields, A. C. Wilson, *J. Mol. Evol.* **24**, 212 (1987).
3. W. M. Brown, M. George, A. C. Wilson, *Proc. Natl. Acad. Sci. U.S.A.* **76**, 1967 (1979).
4. T. W. Quinn, *Mol. Ecol.* **1**, 105 (1992).
5. S. Pääbo, *Sci. Am.* **296**, 86 (1993).
6. D. G. Ainley, R. E. LeResche, W. J. L. Sladen, *Breeding Biology of the Adélie Penguin* (Univ. of California Press, Los Angeles, CA, 1983).
7. C. Baroni, G. Orombelli, *Geology* **22**, 23 (1994).
8. Appropriate ancient DNA procedures were employed in a dedicated facility. DNA sequences were deposited in GenBank, with accession numbers AF474792 through AF474887. See the supplemental material (*12*) and Table 2 for details.
9. DNA from blood samples of 380 Adélie penguins was isolated by means of standard procedures. PCR products were sequenced with the PRISM BigDye Terminator sequencing kit (Applied Biosystems) and analyzed on a 377A automated sequencer (Applied Biosystems) [see the supplemental material (*12*)]. DNA sequences were deposited in GenBank, with accession numbers AF474412 through AF474791.
10. H.-J. Bandelt, V. Macauley, M. Richards, *Mol. Phyl. Evol.* **16**, 8 (2000).
11. C. Baroni, G. Orombelli, *Quat. Res.* **36**, 157 (1991).
12. Supplemental material, including details of the ^{14}C-dated material and latitude and longitudinal coordinates of each sampling location, is available on *Science* Online at www.sciencemag.org/cgi/content/full/295/5563/2270/DC1 or at www.massey.ac.nz/dmlamber.
13. N. Metropolis, A. Rosenbluth, M. Rosenbluth, A. Teller, E. Teller. *J. Chem. Phys.* **21**, 1087 (1953).
14. W. K. Hastings, *Biometrika* **57**, 97 (1970).
15. A. J. Drummond, G. K. Nicholls, A. G. Rodrigo, W. Solomon, *Genetics*, in press.
16. For details of the MCMC methods used, see the supplemental material (*12*). Software for implementing these methods is available at www.cebl.auckland.ac.nz/mepi/index.html.
17. A. Drummond, A. G. Rodrigo, *Mol. Biol. Evol.* **17**, 1807 (2000).
18. J. Felsenstein, *Genet. Res. Cambr.* **59**, 139 (1992).
19. C.-I. Wu, W.-H. Li, *Proc. Natl. Acad. Sci. U.S.A.* **82**, 1741 (1985).
20. J. Felsenstein, *J. Mol. Evol.* **17**, 368 (1981).
21. J. Jouzel *et al.*, *Nature* **364**, 403 (1987).
22. J. R. Petit *et al.*, *Nature* **399**, 429 (1999).
23. E. A. Hadly, M. H. Kohn, J. A. Leonard, R. K. Wayne, *Proc. Natl. Acad. Sci. U.S.A.* **95**, 6893 (1998).
24. J. A. Leonard, R. K. Wayne, A. Cooper, *Proc. Natl. Acad. Sci. USA* **97**, 1651 (2000).
25. T. J. Parsons *et al.*, *Nature Genet.* **15**, 363 (1997).

26. Supported by a Marsden grant to D.M.L. We gratefully acknowledge support from Massey University, Pisa University, the Italian Antarctic Research Programme, NSF, Antarctica New Zealand, and the U.S. Coast Guard. In addition, we thank P. Barrett, A. R. Bellamy, T. J. H. Chin, A. Cooper, L. Davis, S. Eyton, R. Forsberg, J. Heine, M. Hendy, K. Huber, K. Kerry, P. Lockhart, R. Marshall, L. Matisoo-Smith, V. Moulton, V. E. Neall, K. Newman, D. Penny, J. Robins, A. G. Rodrigo, L. Shepherd, P. Stapleton, C. Vleck, R. Ward, and E. C. Young. P.A.R. acknowledges the support of a Massey University doctoral scholarship. B.R.H. acknowledges A. Dress and the Program for Scientific and Technological Exchange between New Zealand and Germany. A.J.D. acknowledges a New Zealand Foundation for Research Science and Technology Bright Future Scholarship and research support from an NIH grant.

15 November 2001; accepted 14 February 2002

A Common Rule for the Scaling of Carnivore Density

Chris Carbone[1]* and John L. Gittleman[2]

Population density in plants and animals is thought to scale with size as a result of mass-related energy requirements. Variation in resources, however, naturally limits population density and may alter expected scaling patterns. We develop and test a general model for variation within and between species in population density across the order Carnivora. We find that 10,000 kilograms of prey supports about 90 kilograms of a given species of carnivore, irrespective of body mass, and that the ratio of carnivore number to prey biomass scales to the reciprocal of carnivore mass. Using mass-specific equations of prey productivity, we show that carnivore number per unit prey productivity scales to carnivore mass near −0.75, and that the scaling rule can predict population density across more than three orders of magnitude. The relationship provides a basis for identifying declining carnivore species that require conservation measures.

Across communities in plants and animals, there is an inverse relationship between population density and body size, such that resource use and availability are driving consistent statistical patterns (*1*–*5*). The critical factor is the individual species' rate of resource use. Typically, resource use is identified in general metabolic or physiological terms, as these represent the invariant properties of all biological systems at different levels. The precise measure and form of resource use have only been described indirectly (*6*–*9*).

We developed a general model (*10*) to predict carnivore density relative to resourc-

[1]Institute of Zoology, Zoological Society of London, Regent's Park, London NW1 4RY, UK. [2]Department of Biology, Gilmer Hall, University of Virginia, Charlottesville, VA 22904, USA.

*To whom correspondence should be addressed. E-mail: chris.carbone@ioz.ac.uk

es, expressed as prey biomass and prey productivity (*11–14*). We tested this model with data from the literature on density of 25 species of carnivores (*15–20*) and their most common prey (*21*) (Table 1). For each species, we calculated the average number of carnivores per unit prey biomass (i.e., carnivore number per 10,000 kg of prey). Controlling for prey biomass allows us to account for the wide variation in carnivore density resulting from variation in prey density within species, as well as to make comparisons between species.

Within carnivore species, population density is typically positively correlated with prey biomass (Fig. 1). In keeping with the assumption that a species' population density is influenced by individual rates of resource use (*4*), the number of carnivores supported on a given biomass of prey increases with decreasing body size. Comparing between species, we find a strong negative relationship between the number of carnivores per 10,000 kg of prey and carnivore body mass (Fig. 2A). The relationship takes the form of a power function [number per 10,000 kg of prey = 89.1 × (carnivore mass)$^{-1.05}$; N = 25, R^2 = 0.83, $P < 0.0001$]. The exponent does not differ significantly from –1.0 [95% confidence limits, –0.845 (upper), –1.25 (lower); confidence limits for constant, 169 (upper), 47 (lower)] (*22–24*).

Our results depend on controlling for prey biomass. A plot of average carnivore population density (number per 100 km^2) against carnivore body mass has considerably more variation than in the biomass-based analyses (Fig. 2B) [number per 100 km^2 = 197.6 × (carnivore mass)$^{-0.88}$; N = 25, R^2 = 0.63, $P < 0.0001$; confidence limits for exponent, –0.59 (upper), –1.18 (lower); confidence limits for constant, 500 (upper), 78 (lower)].

An example of the importance of controlling for prey biomass can be seen by comparing the European badger (*Meles meles*) (*15*) and the coyote (*Canis latrans*) (*19*), both of which weigh about 13 kg. These species differ in average population density by a factor of almost 20, but this is due to a nearly 40-fold difference in the prey biomass density available to these species. Our biomass-based estimate of population density differs by a factor of only 1.6 (Table 1).

Previous studies have pointed out that density estimates of different-sized species may be confounded by sampling area (*25, 26*). Although the density values for carnivores and their prey may both be influenced by the sampling area, it is unlikely that this factor would bias our estimates of the predator-prey relationships in a way that would influence the overall allometric relationship shown in Fig. 2A. In addition, previous analyses of wolf population data (*27*) (Table 1) found that the inclusion of sampling area in a multiple regression model did not substantially improve the model fit.

Ultimately, predator populations are sustained by population productivity rates of their prey rather than by standing biomass. Estimates of turnover on a population-by-population basis are not available, but biomass-based population productivity measures have been estimated in relation to body mass (*11–13*). We expected that the number of carnivores per unit prey biomass would vary with (carnivore mass)$^{-1.0}$ and that the carnivore number per unit productivity would vary with (carnivore mass)$^{-0.75}$ (*10*). We plotted the average ratio of carnivore number per unit productivity (number per 10,000 kg per year) against carnivore mass (Fig. 2C). This relationship has an exponent not significantly different from –0.75 [number per unit productivity = 56.2 × (carnivore mass)$^{-0.66}$; N = 24, R^2 = 0.70, $P < 0.0001$; exponent confidence limits, –0.48 (upper), –0.85 (lower); confidence limits for constant, 101 (upper), 31 (lower)] (*28*). These findings support the notion that there is no systematic variation in prey productivity between carnivore species, and that carnivore density is constrained by metabolic rates and prey abundance.

We selected species that provide a range of body sizes, habitats, and feeding strategies; these include an invertebrate-feeder [the European badger (*15*)] and vertebrate hunter

Table 1. Summary of carnivore density and prey biomass. The number of carnivores per 10,000 kg of prey biomass was estimated from the ratio of carnivore population density (number per 100 km^2) to biomass density (in units of 10,000 kg per 100 km^2) of the main prey species averaged for each species. These values were used in Fig. 2A. Minimum and maximum estimates of the carnivore density and prey biomass density obtained for this study are provided (*43*).

Carnivore species	Average mass (kg)	Number of populations	Carnivore density		Prey biomass (10,000 kg per 100 km^2)
			Number per 10,000 kg of prey biomass (species average)	Number per 100 km^2	
Least weasel* (*Mustela nivalis*)	0.14	6	1656.49	183.67 to 8000.00	0.24 to 8.33
Ermine (*Mustela erminea*)	0.16	2	406.66	105.00 to 1333.33	0.38 to 2.47
Small Indian mongoose (*Herpestes javanicus*)	0.55	3	514.84	1300.00 to 2850.00	3.00 to 5.00
Pine marten (*Martes martes*)	1.3	1	31.84	56.80	1.78
Kit fox (*Atelocynus microtis*)	2.02	2	15.96	16.00 to 24.00	0.66 to 3.05
Channel Island fox (*Urocyon littoralis*)	2.16	1	145.94	957	6.56
Arctic fox (*Alopex lagopus*)	3.19	14	21.63	2.22 to 28.57	0.01 to 28.11
Red fox (*Vulpes vulpes*)	4.6	2	32.21	10.00 to 112.00	1.19 to 2.00
Bobcat (*Lynx rufus*)	10.0	1	9.75	3.40	0.35
Canadian lynx* (*Lynx canadensis*)	11.2	26	4.79	1.99 to 22.59	0.17 to 13.86
European badger (*Meles meles*)	13.0	8	7.35	110.00 to 840.00	6.20 to 714.00
Coyote* (*Canis latrans*)	13.0	16	11.65	2.29 to 44.44	0.35 to 14.85
Ethiopian wolf (*Canis simensis*)	14.5	2	2.70	19.00 to 120.00	25.00 to 31.34
Eurasian lynx (*Lynx lynx*)	20.0	2	0.46	0.98 to 2.90	2.31 to 5.90
Wild dog (*Lycaon pictus*)	25.0	10	1.61	0.07 to 15.00	0.16 to 110.00
Dhole (*Cuon alpinus*)	25.0	2	0.81	13.00 to 30.00	17.05 to 34.94
Snow leopard (*Uncia uncia*)	40.0	1	1.89	5.75	3.04
Wolf (*Canis lupus*)	46.0	23	0.62	0.50 to 4.20	0.89 to 8.10
Leopard (*Panthera pardus*)	46.5	19	6.17	0.50 to 37.04	0.03 to 41.63
Cheetah (*Acinonyx jubatus*)	50.0	7	2.29	0.61 to 7.79	0.16 to 6.69
Puma (*Puma concolor*)	51.9	3	0.94	0.37 to 7.00	1.00 to 11.00
Spotted hyena (*Crocuta crocuta*)	58.6	12	0.68	0.59 to 184.19	1.26 to 121.46
Lion (*Panthera leo*)	142.0	21	3.40	0.80 to 38.50	0.01 to 116.99
Tiger (*Panthera tigris*)	181.0	6	0.33	0.70 to 15.84	4.00 to 89.54
Polar bear* (*Ursus maritimus*)	310.0	8	0.60	0.28 to 2.11	0.42 to 3.37

*Includes more than one population estimate from the same area in relation to annual changes in prey density.

specialists [e.g., the African lion (*Panthera leo*) (*16*), leopard (*Panthera pardus*) (*16, 17*), and polar bear (*Ursus maritimus*) (*18*)]. Despite the wide variation in species' ecology, we find remarkable consistency in the average population density in relation to prey biomass and carnivore mass. However, some of the residual variation in population density can be explained in terms of species' biology. For example, interspecific predation and competition is a major factor influencing carnivore population density (*29*). African wild dogs (*Lycaon pictus*) and cheetahs (*Acinonyx jubatus*) can be found at lower densities in areas where prey are very abundant because of the abundance of competing lions and spotted hyenas in these areas (*30, 31*).

Clearly, all species are influenced to some degree by competition with other carnivores, and this must contribute to the variation found in density estimates across populations. Furthermore, the temporal responses of carnivore density to changes in prey may be somewhat related to turnover rates in different-sized prey (*29*). Lynx (*Lynx canadensis*) and coyotes (*Canis latrans*) feeding primarily on smaller prey such as rodents and hares show more rapid functional responses than do larger carnivores such as Isle Royale wolves (*Canis lupus*), which require 3 to 5 years to respond to population changes in moose numbers (*29*). As more data become available, our predictive model should be refined to quantitatively show the effect of these ecological differences in species abundance.

Allometric scaling, frequently used in biology to extrapolate trait values for species that are relatively unknown, is increasingly being applied to the prediction of population numbers for rare, endangered, and threatened species (*32–34*). Scaling studies that control for key ecological variables (such as resource availability) may provide an important framework for identifying species that deviate from expected values because of other ecological processes. The data on the Eurasian lynx cited in this study provide an example (Fig. 2A). This species is rare relative to the estimated prey biomass availability (*35–37*). One population was recently reintroduced and both populations have been exposed to poaching, possibly contributing to the relatively low densities at these sites.

Mammalian carnivores are often uniquely characterized by fine-tuned relationships with their prey (*38–40*). It appears that carnivores are closely tied not only to prey size (*14*) but also to prey biomass. Carnivore populations and species are now rapidly dwindling in numbers. At least 90 carnivore species are currently listed as threatened or endangered (*41*). Our results show that prey density is a fundamental determinant of carnivore density both within and between species. Given that carnivore population density has been identified as a predictive factor influencing extinction risk (*42*), prey density is critical to the future of stable carnivore populations.

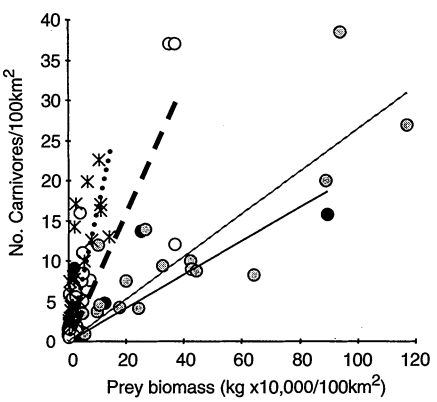

Fig. 1. Carnivore density (number per 100 km^2) plotted against prey biomass density (in units of 10,000 kg per 100 km^2) for different species of carnivores. For the purposes of illustration, we show the slopes of the regression (plotted through the origin) estimated for each species (see text for details): solid circles and solid line, tiger (*Panthera tigris*); shaded circles and gray line, lion (*Panthera leo*); open circles and dashed line, leopard (*Panthera pardus*); asterisks and dotted line, Canadian lynx (*Lynx canadensis*).

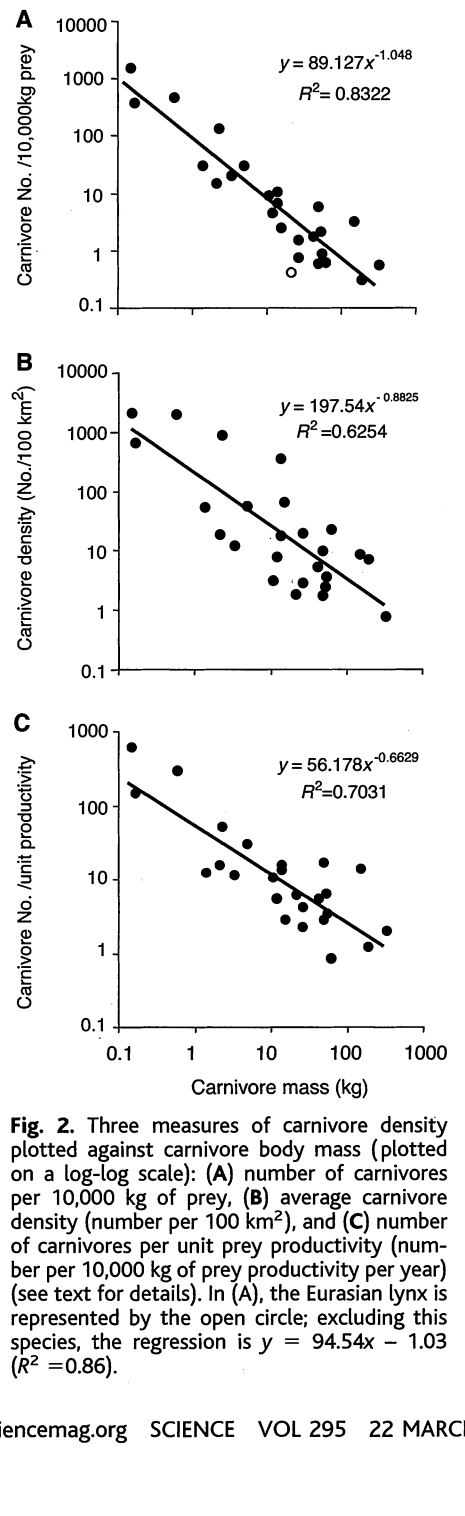

Fig. 2. Three measures of carnivore density plotted against carnivore body mass (plotted on a log-log scale): (**A**) number of carnivores per 10,000 kg of prey, (**B**) average carnivore density (number per 100 km^2), and (**C**) number of carnivores per unit prey productivity (number per 10,000 kg of prey productivity per year) (see text for details). In (A), the Eurasian lynx is represented by the open circle; excluding this species, the regression is $y = 94.54x - 1.03$ ($R^2 = 0.86$).

References and Notes

1. P. A. Marquet, *Science* **289**, 1487 (2000).
2. J. H. Brown, *Macroecology* (Univ. of Chicago Press, Chicago, 1995).
3. J. H. Brown, G. B. West, B. J. Enquist, in *Scaling in Biology: Patterns, Processes, Causes and Consequences*, J. H. Brown, G. B. West, Eds. (Oxford Univ. Press, Oxford, 2000), pp. 1–24.
4. B. J. Enquist, J. H. Brown, G. B. West, *Nature* **395**, 163 (1998).
5. J. Damuth, *Nature* **290**, 699 (1981).
6. _____, *Nature* **395**, 115 (1998).
7. F. Magnani, *Nature* **398**, 572 (1999).
8. B. J. Enquist, J. H. Brown, G. B. West, *Nature* **398**, 573 (1999).
9. R. C. Dewar, *Nature* **398**, 572 (1999).
10. Following (*4–6*), maximum population size (*Nmax*) for species *i* can be expressed as

$$Nmax_{ij} = a \times (R_j/Mb_i^b)$$

where Mb_i^b represents the mass related metabolic rate (typically, $b \approx 0.75$) of species *i* in population *j* (assuming body mass is constant across populations), R_j represents the resources available to the population *j*, and *a* is a constant. We compiled data from studies that had estimates of both carnivore and prey density. We approximated R_j for each carnivore population *j* by (i) calculating the prey biomass per 100 km^2 [multiplying species weight (kg) by species density (number per 100 km^2)], and (ii) calculating for each species the mass-specific productivity per unit biomass (*11–13*). The average ratios of carnivore density (number per 100 km^2) to prey biomass (in units of 10,000 kg per 100 km^2) and carnivore density to prey productivity (in units of 10,000 kg per 100 km^2 per year) were calculated across populations for each carnivore species. The productivity/biomass ratio typically varies with $(\text{mass})^{-0.25}$ (*13*), indicating that productivity is independent of body mass (*5, 6*). The ratio of carnivore number to prey productivity $[(\text{mass})^{-0.75}/(\text{mass})^0]$ should then simply scale as $(\text{mass})^{-0.75}$, the exponent representing the inverse of the metabolic rate (*b*).
11. J. O. Farlow, *Ecology* **57**, 841 (1976).
12. K. Banse, S. Mosher, *Ecol. Monogr.* **50**, 355 (1980).
13. R. H. Peters, *The Ecological Implications of Body Size* (Cambridge Univ. Press, Cambridge, 1983).
14. C. Carbone, G. M. Mace, S. C. Roberts, D. W. Macdonald, *Nature* **402**, 286 (1999).
15. H. Kruuk, T. Parish, *J. Zool.* **196**, 31 (1982).
16. R. East, *Afr. J. Ecol.* **22**, 245 (1984).
17. T. N. Bailey, *The African Leopard—Ecology and Behavior of a Solitary Felid* (Columbia Univ. Press, New York, 1993).
18. I. Stirling, N. A. Oritsland, *Can. J. Fish Aquat. Sci.* **52**, 2594 (1995).
19. M. Odonoghue, S. Boutin, C. J. Krebs, E. J. Hofer, *Oikos* **80**, 150 (1997).
20. A. Angerbjorn, M. Tannerfeldt, S. Erlinge, *J. Anim. Ecol.* **68**, 34 (1999).
21. The most common prey species were usually identified in the literature (*43*) and constituted 70% or more of the diet. Where prey biomass was not estimated, species weights were multiplied by species density.
22. In a multivariate analysis, we find that carnivore density is significantly related to prey biomass but

not to carnivore mass ($F = 26.94$; $df = 2, 22$; $P < 0.0001$; prey biomass: $F = 6.42$, $P < 0.016$; body mass: $F = 0.26$, not significant). Controlling for phylogeny (*23*, *24*), we get a similar result: ln(number per 10,000 kg of prey) + 1 = −1.12 × ln(carnivore mass); $r = 0.753$, $P < 0.01$. One contrast in the body mass and prey biomass analysis was excluded, calculated between *Lynx* and *Panthera*, because it had a Studentized deleted residual greater than 3.

23. A. Purvis, A. Rambaut, *Comput. Appl. Biosci.* **11**, 247 (1995).
24. O. R. P. Bininda-Edmonds, J. L. Gittleman, A. Purvis, *Biol. Rev.* **74**, 143 (1999).
25. K. S. Smallwood, C. Schonewald, *Oecologia* **105**, 329 (1996).
26. T. M. Blackburn, K. J. Gaston, *Oikos* **75**, 303 (1996).
27. T. K. Fuller, D. L. Murray, *Anim. Conserv.* **1**, 153 (1998).
28. Controlling for phylogeny yields the following expression: ln(number per productivity) = −0.36 × ln(carnivore mass); $r = 0.449$, $P < 0.05$. The contrast between canids and felids had a large leverage and was removed.
29. T. K. Fuller, P. R. Sievert, in *Carnivore Conservation*, J. L. Gittleman, S. M. Funk, D. W. Macdonald, R. K. Wayne, Eds. (Cambridge Univ. Press, Cambridge, 2001), pp. 163–178.
30. M. G. L. Mills, M. L. Gorman, *Conserv. Biol.* **11**, 1397 (1997).
31. K. M. Laurenson, N. Wielebnowski, T. M. Caro, *Conserv. Biol.* **9**, 1329 (1995).
32. W. A. Calder, in *Scaling in Biology: Patterns, Processes, Causes and Consequences*, J. H. Brown, G. B. West, Eds. (Oxford Univ. Press, Oxford, 2000), pp. 297–323.
33. K. J. Gaston, T. M. Blackburn, *Patterns and Processes in Macroecology* (Blackwell Scientific, Oxford, 2000).
34. S. P. Hubbell, *The Unified Neutral Theory of Biodiversity and Biogeography* (Princeton Univ. Press, Princeton, NJ, 2001).
35. A. Molinari-Jobin, P. Molinari, C. Breitenmoser-Würsten, U. Breitenmoser, *Wildlife Biol.*, in press.
36. A. Jobin, P. Molinari, U. Breitenmoser, *Acta Theriol.* **45**, 243 (2000).
37. B. Jedrzejewski, W. Jedrzejewski, *Predation in Vertebrate Communities: The Baialowieza Primeval Forest as a Case Study* (Springer-Verlag, Berlin, 1998).
38. A. F. Vezina, *Oecologia* **67**, 555 (1985).
39. J. L. Gittleman, M. E. Gompper, *Science* **291**, 997 (2001).
40. J. Berger, J. E. Swanson, I. L. Persson, *Science* **291**, 1036 (2001).
41. C. Hilton-Taylor (Compiler), *2000 IUCN Red List of Threatened Species* (IUCN–The World Conservation Union, Gland, Switzerland, 2000).
42. A. Purvis, J. L. Gittleman, G. Cowlishaw, G. M. Mace, *Proc. R. Soc. London Ser. B***267**, 1947 (2000).
43. A version of the table with a full list of references can be found at *Science* Online at www.sciencemag.org/cgi/content/full/295/5563/2273/DC1.
44. We thank K. Gaston, J. Brown, K. Jones, P. Bennett, S. Funk, M. Rowcliffe, C. Mueller, A. Bourke, G. Mace, T. Coulson, S. Semple, J. Du Toit, J. Fulford, I. J. Gordon, and three anonymous referees for helpful discussions and comments on earlier drafts of the manuscript. We are grateful to the following for access to data: A. Jobin, Z. T. Ashenafi, K. Murphy, S. Roy, A. Venkataraman, A. T. Johnsingh, A. Angebjorn, and T. Coonan.

13 November 2001; accepted 21 January 2002

Neuronal Calcium Sensor 1 and Activity-Dependent Facilitation of P/Q-Type Calcium Currents at Presynaptic Nerve Terminals

Tetsuhiro Tsujimoto,[1]*† Andreas Jeromin,[2]* Naoto Saitoh,[1] John C. Roder,[2] Tomoyuki Takahashi[1]

P/Q-type presynaptic calcium currents (I_{pCa}) undergo activity-dependent facilitation during repetitive activation at the calyx of the Held synapse. We investigated whether neuronal calcium sensor 1 (NCS-1) may underlie this phenomenon. Direct loading of NCS-1 into the nerve terminal mimicked activity-dependent I_{pCa} facilitation by accelerating the activation time of I_{pCa} in a Ca^{2+}-dependent manner. A presynaptically loaded carboxyl-terminal peptide of NCS-1 abolished I_{pCa} facilitation. These results suggest that residual Ca^{2+} activates endogenous NCS-1, thereby facilitating I_{pCa}. Because both P/Q-type Ca^{2+} channels and NCS-1 are widely expressed in mammalian nerve terminals, NCS-1 may contribute to the activity-dependent synaptic facilitation at many synapses.

Neurotransmitter release is triggered by Ca^{2+} influx through presynaptic voltage-dependent Ca^{2+} channels (*1*). Modulation in the presynaptic calcium current (I_{pCa}) results in robust alteration of synaptic efficacy because of their nonlinear relationship (*2*). At the calyx of Held nerve terminal, repetitive activation of Ca^{2+} channels increases the amplitudes of I_{pCa} (*3–5*). The magnitude of I_{pCa} facilitation is dependent on the extracellular Ca^{2+} concentration and is attenuated by intraterminal loading of Ca^{2+} chelating agents (*4*, *5*). This I_{pCa} facilitation is distinct from the voltage-dependent relief of Ca^{2+} channels from tonic inhibition by heterotrimeric guanine nucleotide binding (G) proteins (*6*, *7*), because presynaptic loadings of guanine nucleotide analogs have no effect (*4*). A Ca^{2+}-binding protein may thus be involved in the activity-dependent I_{pCa} facilitation.

Among neuron-specific Ca^{2+}-binding proteins, frequenin was first cloned from *Drosophila T(X;Y) V7* mutants (*8*). Later, the frequenin homolog NCS-1 was cloned from a variety of species (*9–14*). NCS-1 (frequenin) is widely expressed in neuronal somata, dendrites, and nerve terminals (*14–18*) throughout embryonic and postnatal development (*14*, *17*). Overexpression (*19*) or intracellular loading of NCS-1 in motoneurons (*10*) enhances neuromuscular transmission. We investigated whether NCS-1 is involved in the activity-dependent I_{pCa} facilitation at the calyx of Held synapse.

Whole-cell voltage-clamp recordings were made from a calyceal nerve terminal (*20*), and I_{pCa} was elicited by an action potential waveform command pulse at 0.1 Hz. The half-width and the peak amplitude of a prerecorded action potential were similar to those reported for afferent fiber–stimulated action potentials in 14-day-old rats (*21*). After a stable epoch of I_{pCa}, NCS-1 was infused into a nerve terminal through a perfusion tube (Fig. 1A). After infusion, amplitudes of I_{pCa} gradually increased, reached a maximum in 5 min, and then gradually declined. This decline may be caused by "adaptation" in the mechanism of facilitation by NCS-1, because I_{pCa} elicited at 0.1 Hz does not undergo rundown for more than 20 min (*22*). The mean magnitude of I_{pCa} facilitation 5 min after the onset of NCS-1 infusion was 113 ± 37% (mean ± SEM, $n = 3$).

We next examined the effect of NCS-1 on I_{pCa} elicited by a 5-ms depolarizing pulse. When NCS-1 was included in the presynaptic pipette solution, the rise time of I_{pCa} was significantly faster than rise times in the presence of heat-inactivated (H.I.) NCS-1 or in the absence of NCS-1 [Fig. 1, B (inset) and C]. The current-voltage (*I-V*) relationship of I_{pCa} measured at 1 ms after the onset of the command pulse had a peak at –10 mV in the presence of NCS-1, whereas the peaks were at 0 mV in the presence of H.I. NCS-1 or in the absence of NCS-1 (Fig. 1B). Similarly, in the presence of NCS-1, the half-activation voltage ($V_{1/2}$) calculated from the modified Boltzmann equation (*20*) was significantly more negative than those in the presence of H.I. NCS-1 or in the absence of NCS-1 (Fig. 1D). However, NCS-1 had no effect on the magnitude of plateau Ca^{2+} currents (Fig. 1E).

NCS-1 has four helix-to-helix Ca^{2+}-binding architectures (EF-hands) and binds three

[1]Department of Neurophysiology, University of Tokyo Faculty of Medicine, Tokyo 113-0033, Japan. [2]Mount Sinai Hospital Research Institute, Toronto, Ontario M5G 1X5, Canada.

*These authors contributed equally to this work.
†To whom correspondence should be addressed. E-mail: tujimoto-tky@umin.ac.jp